Malignancies of the Pediatric Lower Respiratory Tract

8

R. Paul Guillerman, Esben Vogelius, Alfredo Pinto-Rojas, and David M. Parham

Introduction

Masses of the lungs and lower airways in children have a wide differential diagnosis. Nonneoplastic etiologies are most common and can be congenital, inflammatory, infectious, vascular, or posttraumatic. For example, congenital pulmonary airway malformations (CPAM), granulomatous diseases, abscesses, infarctions, and hematomas can all present as masses. Additionally, pneumonia in childhood can be associated with a round, mass-like consolidation that simulates a neoplasm [1]. Secondary (metastatic) neoplasms involving the lungs are far more common than primary lung neoplasms in children [2].

Evidence-based evaluation of neoplastic masses of the lungs in children is handicapped by the rarity of the disease entities and the paucity of associated literature. The literature is largely composed of case reports, small case series, and reviews. Hartman and Shochat in 1982 summarized 230 cases of primary neoplasms of the lungs in children [3]. Subsequently, Hancock et al. incorporated an additional 153 cases for a review in 1993 [4]. Long-term, single-center reviews by Cohen and Kaschula [2] and subsequently Dishop and Kuruvilla [5] and Yu et al. [6] have contributed further cases to the literature.

R.P. Guillerman, M.D. (✉)
Department of Pediatric Radiology, Texas Children's Hospital, Baylor College of Medicine, 6701 Fannin Street, Suite 470, Houston, TX 77030, USA
e-mail: rpguille@texaschildrens.org

E. Vogelius, M.D.
Cleveland Clinic, Cleveland, OH, USA

A. Pinto-Rojas, M.D.
University of Calgary, Calgary, AB, Canada T2N 1N4

D.M. Parham, M.D.
Children's Hospital Los Angeles, Los Angeles, CA, USA

University of Southern California, Los Angeles, CA, USA

The largest series remains that of Hancock et al. [4]. They reviewed 383 total cases of pediatric primary neoplasms of the lungs from multiple centers. Of these they found 76 % (291/383) to be malignant and 24 % (92/383) to be benign. This preponderance of malignant tumors becomes even greater (88 %, 339/383) if the 48 cases of inflammatory myofibroblastic tumor (IMT), also known as inflammatory pseudotumor, are reclassified as low-grade malignancies per the revised WHO criteria [7].

Benign Tumors

Before being reclassified as a low-grade malignancy, IMT was regarded as the most commonly encountered primary benign neoplasm of the lung in children. The second most common entity was the hamartoma followed by benign neurogenic tumors and leiomyomas [4]. A subsequent series reported the most common benign neoplasm to be the squamous papilloma [5]. Other rarer benign entities include mucous cell adenoma, granular cell tumor, benign teratoma, hemangioma, lymphangioma, chondroma, juvenile xanthogranuloma, lipoblastoma, immature mesenchymal hamartoma, and solitary fibrous tumor [5].

Malignant Tumors

Secondary

Secondary (metastatic) malignant tumors are reported to be five times as common as primary neoplasms [2]. A wide variety of tumors can metastasize to the lungs. Lung metastases are most common in Wilms tumor and osteosarcoma [8]. They can also be seen in Ewing sarcoma, rhabdomyosarcoma, lymphoma/leukemia, hepatocelluar carcinoma, hepatoblastoma, and neuroblastoma. The mechanism of spread is typically hematological dissemination, resulting in well-defined pulmonary nodules. However, lymphatic spread giving a reticular or

D.M. Parham et al. (eds.), *Pediatric Malignancies: Pathology and Imaging*,
DOI 10.1007/978-1-4939-1729-7_8,

miliary pattern can also be seen, notably in lymphoma/leukemia and neuroblastoma [8]. Pulmonary infiltration in the setting of leukemia can demonstrate ill-defined margins more typical of an inflammatory process.

Cavitation can be seen with Wilms tumor, Hodgkin lymphoma, and osteosarcoma metastases which can lead to pneumothorax. Osteosarcoma metastases can also demonstrate a calcified or ossified matrix which is a relatively specific finding [8].

Primary

Primary malignant tumors of the lower respiratory tract are far less common than metastases but will constitute the predominant focus of the remainder of this chapter.

Pleuropulmonary blastoma (PPB) is likely the most common primary malignancy of the lung in childhood. Analysis is somewhat limited by the wide variety of terminologies previously used to refer to this entity. PPB accounted for about 20 % of pediatric primary lung malignancy in the series of Hancock et al. [4]. It is predominantly seen in children less than 6 years of age. It has a varied appearance ranging from cystic to solid. The cystic form is indistinguishable from the more common large cyst form of CPAM by gross inspection or imaging [9].

Bronchogenic carcinoma was reported as the second most common primary lung malignancy by Hancock et al., accounting for 16.8 % of cases [4]. This number may be contaminated by inclusion of older case reports and older patients. More recent single-center experience reports a proportion below 10 % [2, 5, 6]. There are no specific imaging findings of bronchogenic carcinoma but it tends to present at a late stage with poor prognosis (90 % mortality) [10].

Bronchial carcinoid tumor was the next most common primary malignancy of the lower respiratory tract in children and the most common endobronchial tumor, accounting for 16.5 % of pediatric primary lung malignancy in the series of Hancock et al. [4]. Bronchial carcinoids are typically a single endobronchial lesion with variable calcification and enhancement. Uptake of octreotide on somatostatin receptor scintingraphy is specific to this diagnosis [11].

Bronchial mucoepidermoid carcinoma (MEC) was the fourth most common pediatric primary malignancy of the lower respiratory tract and second most common endobronchial tumor, accounting for 13 % of cases in the series of Hancock et al. [4]. The mass was typically of low grade and demonstrated a good prognosis. MEC and other salivary gland tumors were previously referred to as bronchial adenomas.

Other primary malignancies of the lower respiratory tract account for less than 10 % of tumors and include bronchopulmonary fibrosarcoma, rhabdomyosarcoma, leiomyosarcoma, solitary fibrous tumor, plasmacytoma, and immature teratoma [5].

Diagnostic Imaging Modalities

Chest Radiography (CXR)

Chest radiography remains the most common initial imaging modality for evaluation of lung masses secondary to its wide availability, low cost, and relatively low associated radiation dose [12].

Computed Tomography (CT)

Chest CT is used to investigate suspicious or persistent abnormalities seen on CXR, or to detect disease occult on CXR. Compared to CXR, CT is much more sensitive for detecting small lesions and calcifications, and better at defining anatomic relationships and mass effect on critical structures such as the airway and great vessels. Due to its greater sensitivity for small lesions and precision for measuring the size of lesions, CT is routinely used in follow-up of treated malignancy [1]. While CT is highly sensitive, it lacks specificity and cannot reliably differentiate between benign and malignant lung nodules [13, 14]. Correlation with clinical history and serial imaging follow-up improves the specificity. CT is also useful for guiding tissue sampling.

Modern multidetector volumetric CT scanners allow rapid image acquisition, so that the entire chest of a child can be covered in a few seconds or even less than a second, resulting in less motion artifact and less need for sedation. These scanners also permit high-resolution multiplanar image reconstructions and 3D renderings to better depict anatomy for treatment planning. The dose of ionizing radiation from CT is typically much higher than from CXR, but can be reduced by judicious technique and new image reconstruction algorithms [1]. To better characterize tumors and evaluate the mediastinal/hilar structures, intravenous contrast is typically administered for chest CT scans of primary thoracic tumors for initial staging, therapy response assessment, and relapse surveillance. However, chest CT scans performed to detect and follow up lung metastases from extrathoracic tumors can be performed without intravenous contrast without loss of sensitivity [15].

Magnetic Resonance Imaging (MRI)

MRI currently has a limited role in the evaluation of pulmonary malignancy. While there is no associated ionizing radiation exposure, it has a number of disadvantages. It typically requires a relatively long exam time, requiring sedation in infants and most young children. The evaluation of the lung parenchyma is limited by respiratory motion and by the

intrinsically low signal. There may be an adjuvant role for MRI in evaluation of tumors with known or suspected neural foraminal, pericardial, or chest wall extension [12].

Positron Emission Tomography (PET)

Combined fluorodeoxyglucose (FDG)-PET/CT demonstrates increased sensitivity for the detection of small lesions when compared to stand-alone FDG-PET but not when compared to CT. However, there may be a limited role for FDG-PET/CT in adding specificity to the interpretation of small lung nodules or lymph nodes seen by CT [16].

Diagnostic Imaging Strategy

While it is difficult to construct a rigid algorithm for assessing such a heterogeneous group of rare tumors, general imaging guidelines have been proposed [17]. CXR and laboratory analysis remain the initial investigations of choice. If there are suspicious imaging findings, persistent symptoms, or persistent nonspecific radiographic abnormalities, CT should be obtained to detect and define an underlying mass or other causes. Detection of a mass suggestive of neoplasm should prompt biopsy or excision. This approach, in conjunction with increased clinical awareness of these rare but potentially morbid or even fatal conditions, may expedite the diagnosis without unnecessary testing [17].

Normal Lung Development and Malformations

Embryonic lung begins as a foregut diverticulum extending just caudal to the thyroglossal duct during the fourth week of embryogenesis. The growing lung extends into mesenchyme of the upper coelomic cavity, and by epithelial-mesenchymal interaction it forms a progressively complex structure that passes through successive histological phases corresponding to embryo-fetal development. These stages—pseudoglandular, canalicular, saccular, and alveolar—produce a progressively thinner interstitium, an increasingly greater vasculature, and a larger potential air volume. During this process, portions of the original bronchopulmonary diverticulum may pinch off and form bronchogenic cysts, which have tumorlike compressive effects. A variety of malformations including CPAMs are thought to result from in utero bronchial obstruction and resultant lack of proper epithelial-mesenchymal interaction. Type 1 CPAM, a relatively proximal malformation, contains mucinous goblet cells and may give rise to adenocarcinoma in situ and bronchioloalveolar carcinoma [18]. Of note, bronchial malformations often induce striated muscle development rather than the expected smooth muscle, a phenomenon that is recapitulated in pleuropulmonary blastomas (see below).

Specific Neoplasms

Epithelial Malignancies

Unlike lung cancer in adults, epithelial malignancies are extremely rare in children. There are occasional examples, such as the carcinomas that may arise in type 1 CPAM and the epithelial malignancies related to *NUT* fusion genes or human papillomavirus (HPV) infections.

NUT Midline Carcinoma

NUT midline carcinomas are also discussed in the head and neck chapter (Chap. 7).

Definition

Poorly differentiated aggressive carcinoma associated with characteristic rearrangement of the nuclear protein in testes (*NUT*) promoter gene.

Clinical Features and Epidemiology

The largest series of NUT midline carcinomas details 22 cases [19]. No clear gender predilection was present, and the average age of diagnosis was 25 years, although a 78-year-old patient was also affected. The reported age range may suffer from referral bias, as younger patients with undifferentiated carcinoma are more likely to undergo chromosomal analysis/FISH [20]. The presenting symptoms were nonspecific and depended on the primary site of tumor or metastases. Survival was poor with a reported mean survival of 9.5 months [19].

Imaging Features

NUT carcinomas originate from the head, neck, or chest in the majority of cases [19]. Less common origins include the salivary glands [21] and below the diaphragm. Primary sites in the liver, the bladder [22], iliac bone [23], and extremity soft tissues have been reported [24]. The tumor is midline in 70 % of cases [24]. Imaging descriptions of the

tumor are rare. Apart from the midline location, imaging features are nonspecific. On CT, it has been described as heterogeneously low in attenuation with areas of central necrosis. Small areas of central calcification have been reported [24]. On MRI, it appears hypointense on T1-weighted images and mildly hyperintense on T2-weighted images, and enhances heterogeneously with contrast. Both the primary tumor and metastases appear to be FDG-avid on PET. Metastases are frequently widespread. The lungs are the most common site of metastases but metastases to the liver, kidney, brain, spinal cord, and subcutaneous soft tissues have also been reported [24].

Molecular Genetics

NUT midline carcinoma was first described in 1991 by Kubonishi in a patient with suspected thymic carcinoma [25]. On chromosomal analysis the patient was found to have a novel translocation of chromosomes 15 and 19. The site on chromosome 15 was later identified as the *NUT* promoter gene (15q14) that encodes a polypeptide in spermatids, but whose function is unknown. The classic translocation seen in greater than two-thirds of cases occurs with the *BRD4* gene on chromosome 19 that may be involved in chromatin regulation and possibly needed for epithelial differentiation [19]. The translocation can also involve the *BRD3* or other genes and the tumor then referred to as variant NUT midline carcinoma.

Pathology

NUT midline carcinomas typically comprise patternless sheets of primitive, undifferentiated tumor cells, from whence obvious squamous differentiation may abruptly arise [22] (Fig. 8.1). They should be considered Ewing-like small-cell malignancies that lack an *EWS* fusion and strongly express cytokeratin. Immunohistochemical demonstration of nuclear *NUT* expression or FISH testing that indicates *NUT* rearrangement is diagnostic but usually requires use of a specialized center. Because of the multiple fusion partners, RT-PCR is less helpful as a diagnostic tool.

Prognostic Features

With few exceptions, NUT carcinomas are highly lethal malignancies. Most patients die within weeks, as metastases are typically present at diagnosis, and bulky intrathoracic growth produces superior vena cava compression. No association of outcome with fusion type has been demonstrated to date [22].

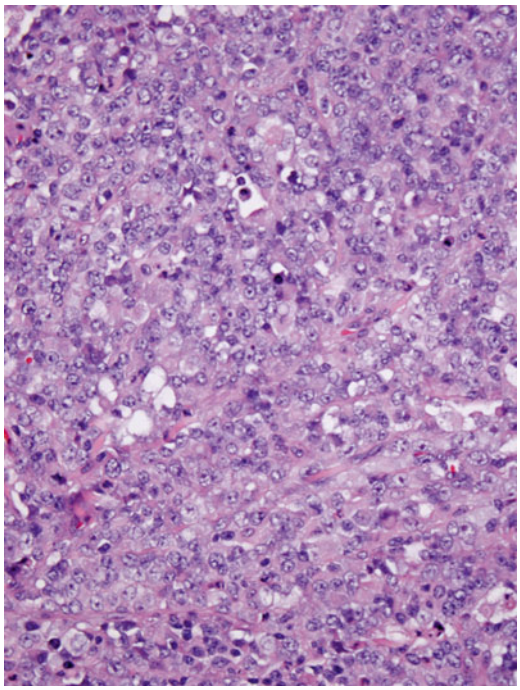

Fig. 8.1 NUT midline carcinoma. Histology consists of an undifferentiated neoplasm with vague epithelioid features

Squamous Cell Carcinoma (SCC)

HPV-related squamous cell carcinomas are discussed in the head and neck chapter (Chap. 7).

Definition

Type of bronchogenic malignancy of the lung.

Clinical Features and Epidemiology

Squamous cell carcinoma (SCC) is a common malignancy in adults, accounting for 44 and 25 % of primary malignancies of the lung of men and women, respectively [26]. In adults there is a strong association with smoking.

Bronchogenic carcinoma is much less common in children than in adults, accounting for 7–17 % of primary pediatric pulmonary malignancies [4, 5]. When seen in children, SCC is often associated with recurrent respiratory papillomatosis (RRP).

RRP is caused by the human papillomavirus (HPV) transmitted primarily via vaginal delivery [27]. RRP is usually isolated to the larynx (>95 % of cases). The distal trachea is affected in less than 5 % of cases and the pulmonary parenchyma is affected in less than 1 % of cases [28]. While pulmonary involvement is uncommon, papillomas are the most

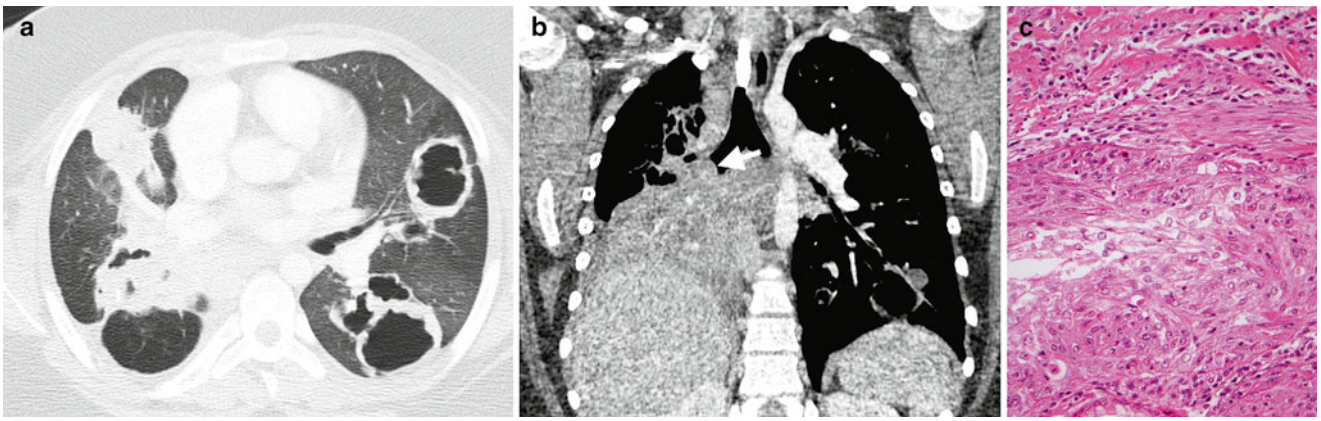

Fig. 8.2 Recurrent respiratory papillomatosis. Axial (**a**) and coronal (**b**) contrast-enhanced chest CT images from a 13-year-old male demonstrate multiple thick-walled cavitary lung lesions and an endobronchial papilloma (*arrow*) occluding the bronchus intermedius with post-obstructive atelectasis of the right middle and lower lobes. Histology (**c**) of another case shows a well-differentiated squamous carcinoma invading the underlying tissues of the bronchial submucosa and inciting adjacent fibrosis

common primary benign tumor of the lower respiratory tract in children (accounting for up to 40 %) [5]. Distal dissemination may be caused by aerogenous embolization of papilloma particles and can be precipitated by tracheotomy or other airway procedures [29]. Juvenile-onset RRP has a bimodal peak at 2 and 10 years of age [30]. No clear sex predilection has been identified.

RRP undergoes malignant transformation into SCC in less than 1 % of cases [28]. Transformation can occur with or without a history of smoking or radiation, and is most frequently observed in males in the third and fourth decades of life.

Imaging Features

RRP can present as a single or, more commonly, multiple masses predominantly affecting the airway and posterior lower lobes [29]. The masses may be solid or cavitary with a thin or thick wall and either air or fluid contents (Fig. 8.2). An air-fluid level is a nonspecific finding that may be seen in the setting of superimposed infection or hemorrhage. Benign lesions may demonstrate increased FDG uptake on PET imaging and simulate malignancy [30]. Findings that suggest malignant transformation include lesion growth, thoracic lymphadenopathy, or distal metastases.

Associated findings include atelectasis, consolidation, and bronchiectasis secondary to airway obstruction and recurrent superimposed infections [29].

Molecular Genetics

Respiratory papillomatosis is usually caused by low-risk HPV types 6 and 11. Certain HPV types, particularly types 16 and 18, are more likely to transform into carcinoma, similar to uterine cervical cancers. With HPV16-associated lesions, transformation is related to genetic polymorphisms or deletions, but aggressiveness of low-risk HPV11-associated lesions does not relate to intratypic variants but rather to the interaction of multiple genetic factors [31].

Pathology

The pathological features of HPV-related carcinomas are discussed in the head and neck chapter (Chap. 7) (Fig. 8.2). Juvenile papillomas from the upper respiratory tract may be aspirated into the bronchial passages. From there, they may act similar to metastatic lesions, as malignant transformation may produce a well-differentiated squamous carcinoma.

Prognostic Features

RRP associated with HPV 11 demonstrates a more aggressive course and worse prognosis [32].

Endobronchial Tumors

Bronchial Carcinoid

Definition

Malignant neuroendocrine tumor of endodermal origin arising from Kulchitsky cells.

Clinical Features and Epidemiology

Neuroendocrine and salivary gland tumors of the tracheobronchial tree were previously referred to as bronchial adenomas [1]. This potentially confusing terminology has fallen

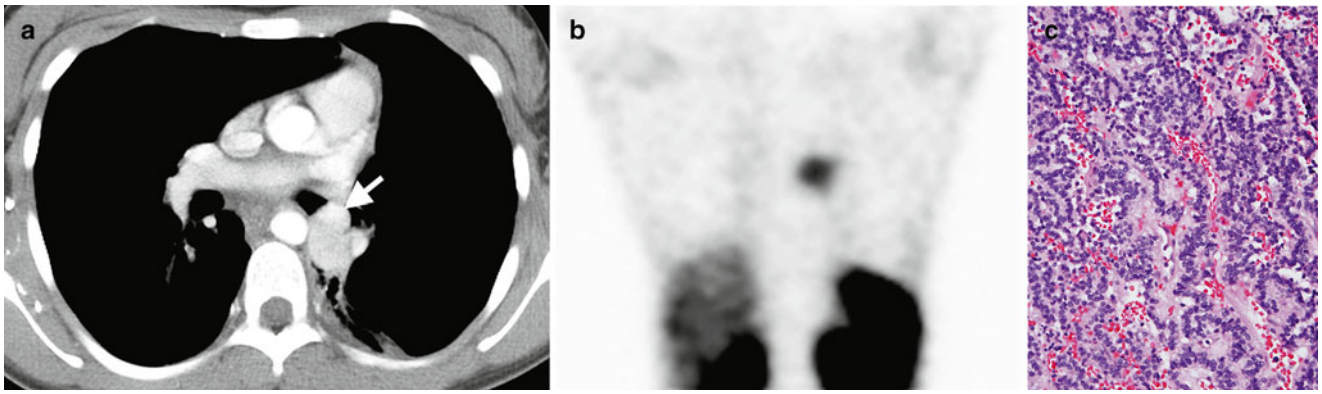

Fig. 8.3 Bronchial carcinoid. An axial contrast-enhanced chest CT image (**a**) from a 13-year-old female shows a hyper-enhancing lobular soft-tissue mass with a "tip of the iceberg" endobronchial component (*arrow*) involving the distal left mainstem bronchus. A coronal image (**b**) from an In-111 octreotide SPECT scan shows radiopharmaceutical uptake by the mass. Histology (**c**) of another case demonstrates uniform cells with round nuclei, forming cords and festoons

out of favor secondary to the variable glandular component and malignant potential of these tumors [33].

Bronchial carcinoid is the most common malignant endobronchial tumor and the second most common primary malignancy of the lower respiratory tract in children (after PPB) [5]. Carcinoids are most commonly seen in the gastrointestinal tract, with only 10–32 % occurring in the tracheobronchial tree [34, 35]. The average age of presentation of bronchial carcinoid is 45–56 years [34, 35]. This is a decade younger than the average age of presentation for other lung malignancies, but carcinoid is still uncommon in the pediatric age range. When it occurs in children, it tends to affect older children and adolescents with the youngest reported patient being 8 years of age [34]. There is no known smoking association, or sex or racial predilection.

Presentation is varied. Post-obstructive atelectasis and pneumonitis are common [35]. Nonspecific respiratory symptoms and signs, including pleuritic pain, dyspnea, cough, wheeze, and hemoptysis, are also seen. The tumor is incidentally detected in up to half of patients. Carcinoid tumors can synthesize a variety of neuroamines and peptides leading to more specific presentations. Overproduction of adrenocorticotropic hormone (ACTH) leads to Cushing syndrome in up to 4 % of patients. Overproduction of serotonin leading to carcinoid syndrome is rare in bronchial carcinoid outside of the setting of metastatic disease (2–5 %). Up to 4 % of carcinoid tumors are associated with other endocrine neoplasias [34]. The most common association is with pituitary tumors, seen in half of this patient subset.

In addition to imaging, detection and follow-up of lesions can be aided by serum and urine 5-hydroxyindolacetic acid (5-HIAA), a serotonin metabolite that is relatively specific though not sensitive for the diagnosis [34].

Imaging Features

The typical appearance of a bronchial carcinoid is that of a single round or lobulated mass that is at least partially endobronchial [35, 36]. The mass is typically 2–5 cm in size. Endoscopy can underestimate the size of the mass as the endobronchial component can represent just the "tip of the iceberg." The mass is seen within the main, lobar, and segmental bronchi in 80 % of cases with a preference for branching sites (Fig. 8.3). The remaining 20 % of bronchial carcinoids are peripheral in location and indistinguishable from intraparenchymal pulmonary masses [35].

In up to 30 % of cases, bronchial carcinoids demonstrate calcification that is best appreciated on CT. The masses demonstrate high signal intensity on T2-weighted MRI images and typically exhibit homogeneous avid enhancement [35]. However, heterogeneous or minimal enhancement does not exclude the entity. Bronchial carcinoids demonstrate octreotide uptake on somatostatin receptor scintingraphy in greater than 86 % of cases [35, 37] (Fig. 8.3).

Associated findings include post-obstructive atelectasis or pneumonitis, bronchiectasis, and mucous plugging. Local or distal recurrence occurs in up to a fifth of cases with 15 % presenting with metastases [35]. Metastases are most commonly seen in the liver, bone, adrenals, and brain.

Molecular Genetics

In the current molecular model [38], bronchial carcinoids originate from bronchial Kulchitsky-type neuroendocrine cells. These cells are capable of producing precursor lesions such as diffuse idiopathic pulmonary cell hyperplasia or tumorlets. Small invasive foci break through the basal lamina and invade locally, producing small lesions termed tumorlets, which are by definition <5 mm in diameter. The most common chromosomal aberrations in pulmonary carcinoids include −11p, +19p, −13q, +19q, +17q. −11p, −6q, +16p, +2-p, and −3p, although these occur at a frequency of <25 % in typical lesions. However, as bronchial carcinoids assume atypical features and undergo carcinomatous transformation, the frequency of these changes rises to as high as 75 % for

−3p and −13q. Approximately 18 % show sporadic mutations and loss of heterozygosity of *MEN1*, the multiple endocrine neoplasia 1 gene.

Pathology

Pulmonary carcinoids generally contain a uniform population of monotonous round cells with regular, central nuclei, granular chromatin, inconspicuous nuclei, and a relatively high nuclear-to-cytoplasmic ratio. The cytoplasm is generally lightly eosinophilic but on occasion is more abundant and resembles that of rhabdoid cells. Rarely, it is clear, and melanin or mucus may be present. Some tumors show marked nuclear pleomorphism, a feature not reliable in predicting behavior. The cells usually grow in an organoid or trabecular pattern, forming nests or cords, but sometimes they form spindle cells or rosettes. The intervening stroma is vascular and collagenous and is capable of producing amyloid, hyaline, bone, or cartilage (Fig. 8.3).

Atypical carcinoids are characterized by the presence of focal necrosis or conspicuous mitotic activity (2–10 mitoses/2 mm^2) [33].

Prognostic Features

Prognostic factors in bronchial carcinoids include stage and the presence of atypical features (atypical carcinoid). Pediatric bronchial carcinoids generally have an excellent long-term outcome with adequate surgery and lymph node excision. Long-term follow-up is required, as relapse may occur years after the initial excision, but usually can be successfully treated with additional surgery [39].

Mucoepidermoid Carcinoma

Definition

Malignant salivary-type neoplasm arising from the mucous cells of the submucosa.

Clinical Features and Epidemiology

Mucoepidermoid carcinoma comprises 0.1–0.2 % of malignant lung tumors and 2.5–7.3 % of endobronchial tumors [34]. While it is even more unusual in children, it is likely the second most common endobronchial malignancy [34]. The tumor has a wide age range of 3–78 years, with half of cases occurring in patients younger than 30. The tumor may be more common in Caucasians and has a 3:2 male-to-female ratio [33].

Obstructive airway symptoms and signs are a common presentation and include wheezing and recurrent pneumonia. Up to 25 % of patients are asymptomatic and the tumor is incidentally discovered [34].

Fig. 8.4 Mucoepidermoid carcinoma. A coronal contrast-enhanced chest CT image from a 12-year-old male depicts a partially calcified endobronchial mass (*arrow*) occluding the left upper lobe bronchus with associated left upper lobe collapse

Mucoepidermoid carcinoma is graded by histology similar to other salivary-type neoplasms into low, intermediate, and high grades. Higher grades have a higher rate of metastasis and worse prognosis [40].

Imaging Features

The typical appearance is a single round, lobulated or polypoid mass occurring in a proximal lobar bronchus [41] (Fig. 8.4). A more peripheral mass with the same histology should raise concern for metastatic salivary gland neoplasm [34]. The mass is typically 1–4 cm in size and often extends beyond the lumen of the bronchus. Calcification is seen in up to half of cases. Grades are indistinguishable by imaging.

These endobronchial tumors frequently cause airway obstruction with associated findings of atelectasis, bronchiectasis, and mucous plugging. Post-obstructive pneumonitis is seen in up to a third of cases [42].

Lymph node extension and distal metastasis are infrequent, being seen in less than 10 % of cases [42].

Molecular Genetics

The molecular genetic features of mucoepidermoid carcinoma are discussed in the head and neck chapter.

Pathology

The pathological features of mucoepidermoid carcinoma are discussed in the head and neck chapter.

Prognostic Features

Pediatric mucoepidermoid carcinomas of the lung are generally low-grade, low-stage lesions with excellent patient survival following excision. In a recent SEER survey [43], all 14 patients survived. In a recent Egyptian study of radiographic features [44], overall survival of patients with salivary gland-type tumors of the lung was affected by the presence of mediastinal/hilar lymphadenopathy, suspected metastatic disease, and primary tumor heterogeneity. Higher FDG uptake on PET was associated with nodal metastasis. The mean survival time for pulmonary mucoepidermoid carcinoma was 4.4 years. In a recent Chinese study [45], prognostic factors for pulmonary mucoepidermoid carcinoma included age, grade, lymph node metastasis, and stage. Lower age had a positive effect on outcome, with 80 % survival in patients <60 years old.

Mesenchymal Tumors

Pleuropulmonary Blastoma

Definition

Pleuropulmonary blastoma (PPB) is a rare primitive mesenchymal, embryonal type neoplasm of the lung and pleura of young children.

Clinical Features and Epidemiology

PPB has been previously termed pulmonary embryoma, pulmonary blastoma, mesenchymal cystic hamartoma, and sarcoma arising in congenital cystic malformations [5]. PPB was described as a tumor distinct from adult pulmonary blastoma in 1988 by Manivel et al. [46]. PPB is a rare neoplasm with approximately 25–50 cases occurring annually in the USA, 500–600 cases reported in the literature, and 370 centrally reviewed cases in the International Pleuropulmonary Registry (Personal communication, Dr. Yoav Messinger, on July 17, 2013). In spite of its rarity, it is likely the most common primary malignancy of the lung in children. Epidemiological data is largely derived from the largest reported case series of 50 patients from the Registry [47]. The average age of presentation is 38 months with the cystic types presenting earlier and rarely presenting at more than 6 years of age. Prenatal presentation of cystic PPB has been reported [48].

There is no apparent sex or racial predilection. About 40 % of patients with PPB or their relatives manifest certain other dysplasias and neoplasms as part of the PPB Family Tumor Dysplasia Syndrome (PPB-FTDS). Conditions associated with PPB-FTDS include PPB, cystic nephroma, pineoblastoma, pituitary blastoma, embryonal rhabdomyosarcoma (especially of the uterine cervix), medulloblastoma, nasal chondromesenchymal hamartoma, ciliary body medulloepithelioma, multinodular goiter, intestinal juvenile hamartomatous polyp, and ovarian stromal sex-cord tumor (especially Sertoli-Leydig tumors) [49–51]. The clinical presentation of PPB ranges from an incidental finding in an asymptomatic patient to nonspecific respiratory or systemic symptoms, such as respiratory distress, fever, chest pain, cough, anorexia, and malaise [47].

Imaging Features

PPB has been categorized into three main types based on gross morphology. Type I is entirely cystic, type II is mixed cystic and solid, and type III is entirely solid [52]. Age of presentation, malignant behavior, and mortality increase with type number. If untreated, progression of type I to type II and III can occur. CPAMs do not transform into PPB [47]. Type I PPB may also spontaneously regress, leading to categorization as type Ir PPB for type I-regressed PPB [49].

Types I and Ir PPB appear as an air-filled unilocular or multilocular thin-walled cyst with delicate septations, and are indistinguishable from the more common large cyst form of CPAM (Fig. 8.5). Findings that favor type I PPB over large-cyst CPAM include the presence of multifocal or bilateral cysts or spontaneous pneumothorax [47–49, 53]. Type II and III PPB usually appear as a large, heterogeneously enhancing mass in the hemithorax with associated mediastinal mass effect and pleural effusion and lack of chest wall invasion [9] (Fig. 8.6). PPB is slightly more common in the right hemithorax than the left, and bilateral tumors may be synchronous or metachronous [54].

Aggressive local invasion of the bronchi, great vessel, and heart is unusual but has been reported [54, 55]. Metastases occur in 11 % and 55 %, respectively, of types II and III cases [49]. The most common location for distal metastasis is the brain, followed by bone. Cerebral metastases are much more frequent in PPB than in other childhood sarcomas [56]. Metastases to the liver, adrenal glands, and ovary have also been reported [47, 49].

Molecular Genetics

Comparative genomic hybridization identifies aberrations (amplifications, gains, losses) in PPB tumors, with DNA gains involving chromosome 8q being the most frequent abnormality. Losses of 9p and 11q are also reported [57]. The sites of gains and losses may contain oncogenes or tumor suppressor genes, respectively.

Children with PPB-FTDS discussed above frequently have heterozygous, germline loss-of-function mutations in the *DICER1* gene that codes for a protein involved in microRNA (miRNA) processing. Loss of DICER 1 function in the epithelium of the developing lung may alter the regulation of diffusible factors that results in mesenchymal proliferation and sarcomatous transformation [58]. DICER1

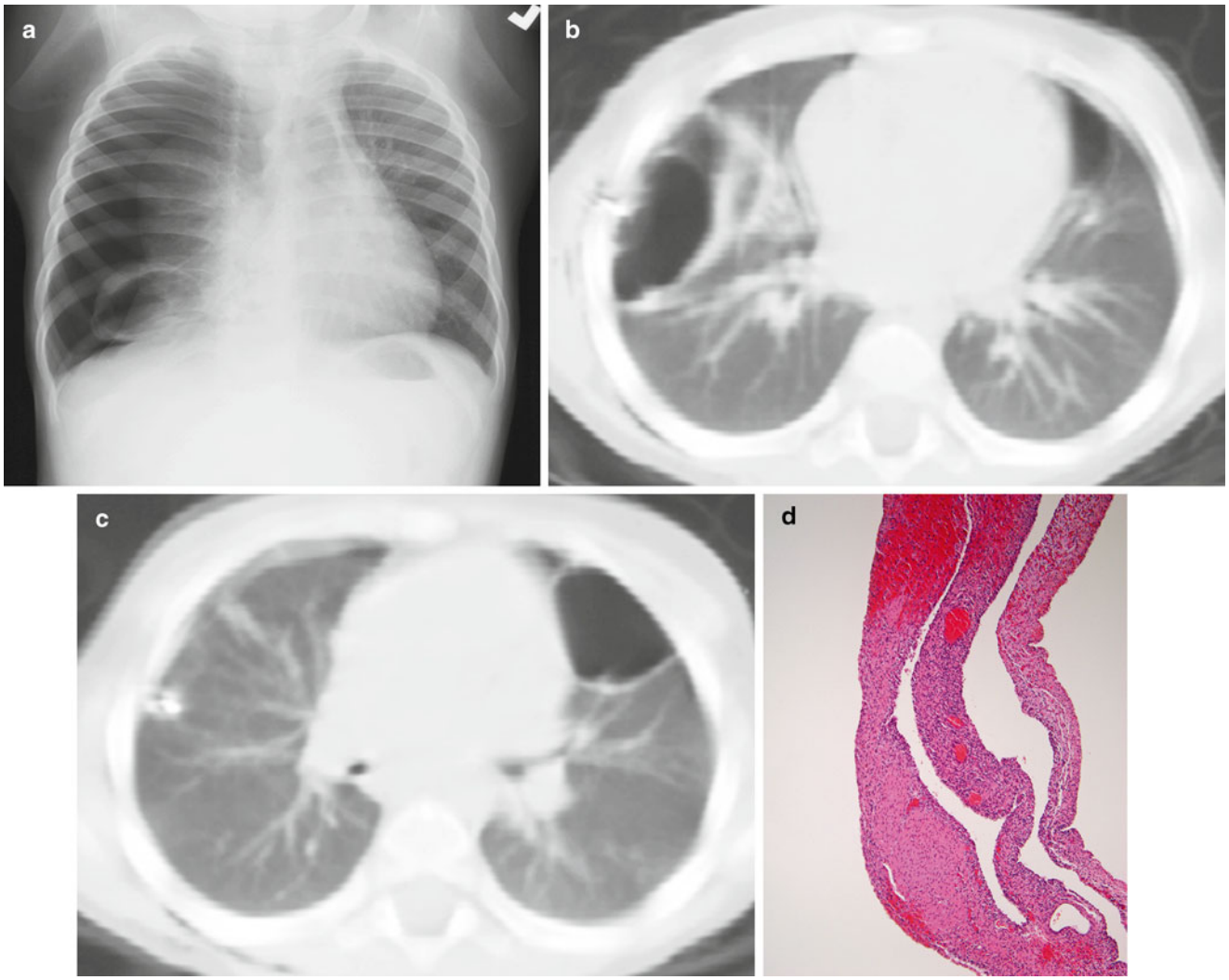

Fig. 8.5 Type I (cystic) pleuropulmonary blastoma. A chest radiograph (**a**) from a 2-year-old presenting with respiratory distress demonstrates a right pneumothorax, right lung collapse, and a cystic lesion of the right lower lung. Axial chest CT images (**b**, **c**) obtained after right chest tube placement and pneumothorax evacuation demonstrate bilateral air-filled, thin-walled cystic lung lesions. Histology (**d**) of another case shows large spaces lined by thin septa, some containing nodules of primitive blastemal cells

mutations are inherited by an autosomal dominant mechanism with variable expressivity, and are thought to be present in 60–70 % of cases of PPB [49].

Pathology

PPB is composed of a malignant mesenchymal component but no malignant epithelial component. It is postulated that PPB originates in mesenchymal elements resembling fetal lung at 10–16 weeks of gestation. Three types (I, II, and III) based on gross morphology are described [59].

A unilocular or multilocular cyst with thin fibrous septa characterizes type I PPB. The cysts are lined by ciliated epithelium with small subepithelial "buds" containing aggregates of primitive mesenchymal cells or nodules of immature cartilage (Fig. 8.5). These small, round-to-spindled, subepithelial mesenchymal cells may display rhabdomyoblastic differentiation. In type Ir (regressed cystic), the small primitive mesenchymal cells are not seen, and the wall or septa of the cyst may be hyalinized or necrotic.

In type II PPB, cystic and plaque-like areas mingle with solid areas with overgrowth of rhabdomyoblasts, spindle cell sarcoma, or blastematous elements. Type III PPB consists of a solid tumor with mixed sarcomatous (fibrosarcoma, rhabdomyosarcoma, pleomorphic undifferentiated sarcoma) and blastematous features (Fig. 8.6). Foci of muscle and chondroid differentiation are frequent, as are foci of anaplasia with giant bizarre pleomorphic tumor cells (Fig. 8.6a). Malignant epithelium is not seen, differentiating PPB from pulmonary blastoma. Immunohistochemical staining is variable from one tissue type to another. Myogenin, desmin, and MyoD1 are useful for the identification of rhabdomyoblasts [49].

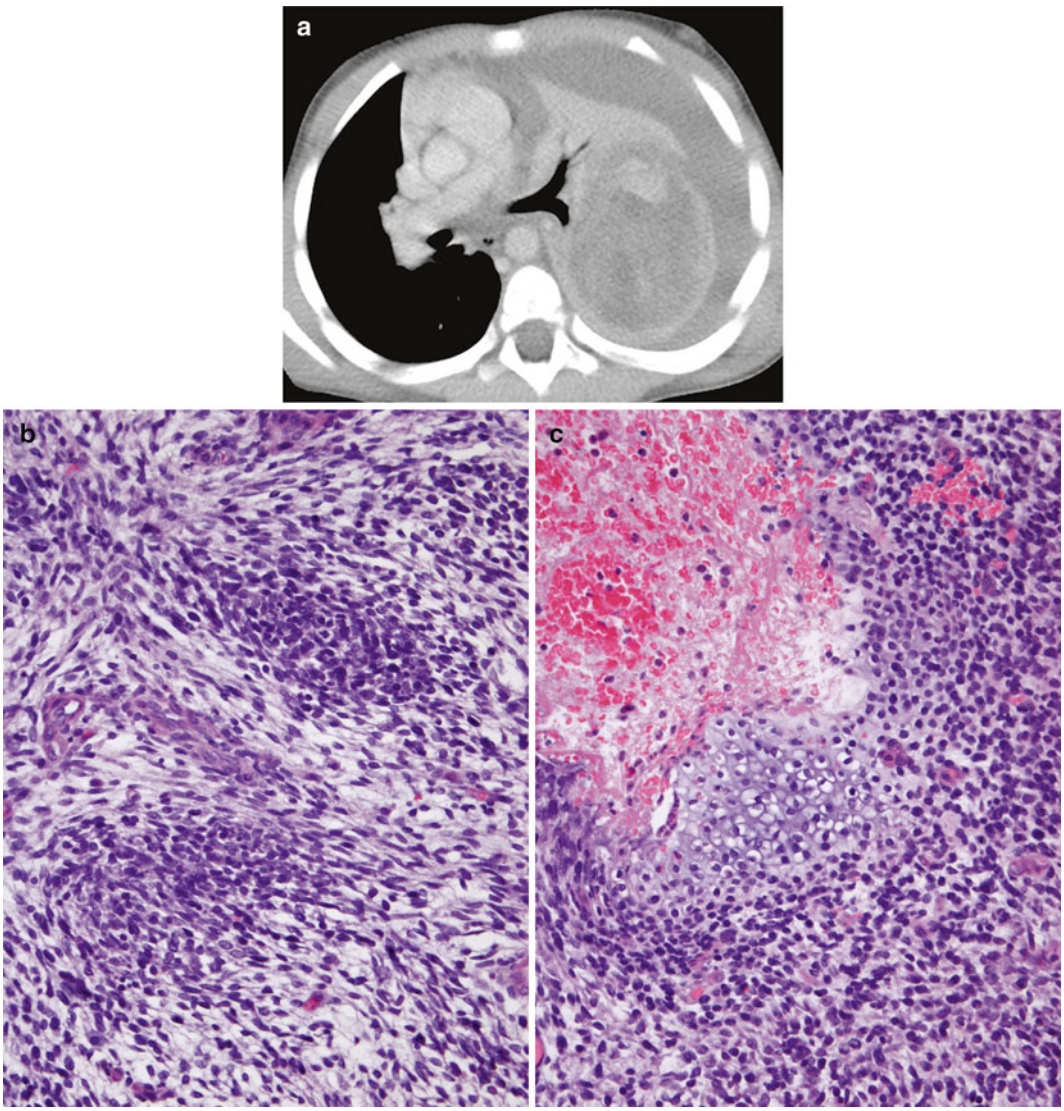

Fig. 8.6 Type III (solid) pleuropulmonary blastoma. An axial contrast-enhanced chest CT image (**a**) from a 3-year-old male reveals a large, heterogeneously enhancing left pulmonary mass with a large left pleural effusion and rightward mediastinal shift from mass effect. Histology (**b**) of another case demonstrates primitive blastemal cells arranged in an organoid pattern. A small bar of hyaloid cartilage is revealed in an additional histologic section (**c**)

As was mentioned, PPB is histologically and clinically distinct from pulmonary blastoma, a rare subtype of malignant biphasic sarcomatoid carcinoma typically seen in adults. However, a recent case report of a neonate described histology distinct from PPB and more similar to adult PB [60]. PB is occasionally reported in adolescents [61].

Prognostic Features

Overall survival rate is estimated at 90 % for type I and 40–60 % for types II and III [49]. Progression of type I to type II and III is well recognized. Tumors do not regress from type III to type II or from type II to type I. Local recurrence develops in fewer than 15 % of type I but is seen in over 45 % of types II and III [49]. Recurrence can affect the ipsilateral or contralateral lung [47]. Sex, tumor side, tumor size, preexisting lung cysts, and extent of surgical resection at the time of diagnosis do not impact prognosis, whereas incomplete resection and extrapulmonary involvement at diagnosis result in a significantly worse prognosis [62].

Fetal Interstitial Lung Tumor (FLIT)

Definition

Tumefactive lesion presenting in utero or early infancy with a solid appearance on imaging and gross inspection and a prominent immature interstitium on histology that resembles immature fetal lung at 20–24 weeks gestational age.

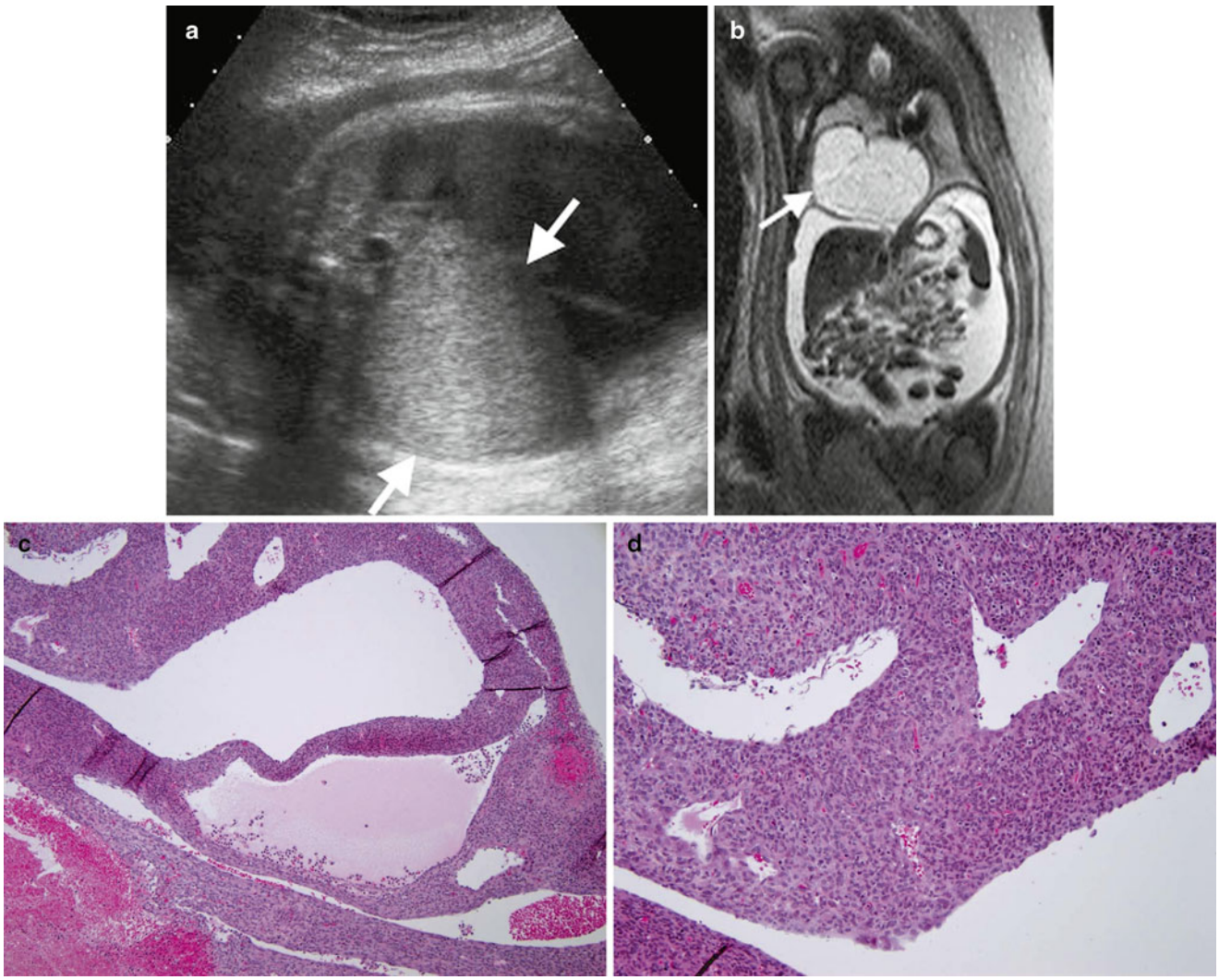

Fig. 8.7 Fetal lung interstitial tumor. Prenatal ultrasound (**a**) at 36 weeks gestation shows a large, well-circumscribed, solid hyperechoic mass arising from the right lung (*arrows*). T2-weighted fetal MRI image (**b**) at 36 weeks gestation shows the high signal intensity mass compressing the adjacent lung and everting the diaphragm, with associated hydrops and large-volume ascites from inferior vena cava compression. Histology (**c**) of another case shows primitive mesenchymal cells that line spaces resembling alveoli. An additional histologic section (**d**) demonstrates constituent cells that are primitive and lack obvious differentiation

Clinical Features and Epidemiology

FLIT is a rare tumor recently described in a series of ten cases [63]. All were discovered before 3 months of age. Two were detected by prenatal ultrasound and one of these was further evaluated by prenatal MRI [64]. In the patient that underwent MRI, the tumor was not seen at routine second trimester prenatal ultrasound but was first noted in late third trimester as a large pulmonary mass causing hydrops, prompting ex utero intrapartum treatment (EXIT procedure) at 37 weeks gestational age. This late gestational growth and late onset of hydrops would be atypical for a CPAM or PPB [64]. The other patients presented with respiratory symptoms, two in the immediate postpartum period [63].

Imaging Features

The tumors are well circumscribed, unifocal, and confined within a single lobe. The tumors have been reported in all lobes, with the right lower lobe being the most common location [63]. The tumors usually appear solid, with small cysts occasionally observed. On prenatal ultrasound, the tumors are hyperechoic compared to normal lung parenchyma (Fig. 8.7). The tumors are predominantly low in attenuation on CT. The single case examined by MRI appeared heterogeneously hyperintense on T2-weighted images, with mass effect compressing the heart and inferior vena cava leading to fetal hydrops (Fig. 8.7). The solid nature of a FLIT can resemble a type 3 CPAM, sequestration, or congenital peribronchial myofibroblastic tumor.

Although rapid growth can be observed, no locally recurrent or metastatic FLIT has been described to date, even in the setting of an incompletely resected lesion [63].

Molecular Genetics

No genetic aberrations have been reported. The one child in the defining series who underwent testing for *DICER1* mutations associated with PPB tested negative [63].

Pathology

Grossly, FLIT manifests as a well-circumscribed solid-to-spongy mass. A fibrous interface demarcates the tumor from adjacent normal lung. Histopathology shows immature airspace-like structures with uniform expansion of immature vimentin-positive interstitial mesenchymal cells with abundant cytoplasmic glycogen (Fig. 8.7). The histology resembles lung arrested in development at 20–24 weeks gestation. The interstitial cells have monotonous, round-to-oval contours and round-to-oval nuclei with a prominent rim of clear-to-pale eosinophilic cytoplasm and well-defined cell borders. Nuclear hyperchromasia, mitoses, or atypia are not identified. Occasional isolated foci of cartilage, similar to that seen in small bronchioles, may be noted [63]. The interstitial cells contain PAS-positive cytoplasm and express vimentin, focal smooth muscle actin, and focal desmin. The epithelial lining of the air spaces is positive for cytokeratin, EMA, and TTF-1.

Prognostic Features

Prognosis is favorable. Resolution of respiratory symptoms and no local recurrence or metastatic disease is expected after resection, even without chemotherapy. In the Dishop et al. series [63], lobectomy or wide resection was performed with complete excision in eight of ten cases. No metastases and no recurrence were reported [63].

Leiomyoma and Leiomyosarcoma

Definition

Spectrum of benign-to-malignant tumors of smooth muscle origin.

Clinical Features and Epidemiology

Primary leiomyoma and leiomyosarcoma of the lung are very rare [10]. An association between human immunodeficiency virus (HIV) infection and both benign and malignant smooth muscle tumors has been noted [65]. While HIV was initially thought to be causative, subsequent studies have shown marked expression of clonal Epstein-Barr virus (EBV) within the tumor cells that is not seen in non-HIV-associated smooth muscle tumors or normal muscle [66]. This is similar to the association of EBV with tumors in patients undergoing solid organ transplant [67]. The causal mechanism of tumorigenesis is not entirely known. The frequency of tumors in the pediatric HIV population is considerably lower than in adults, and no specific age or sex predilection has been noted [65].

Presentation usually consists of nonspecific respiratory signs and symptoms [10]. Given the frequent immunosuppression of these patients, infection is often the initial consideration and definitive diagnosis can be considerably delayed [66].

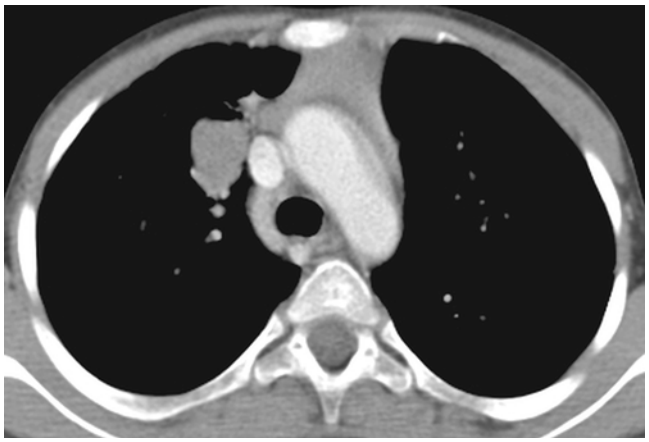

Fig. 8.8 EBV-related smooth muscle tumor. An axial contrast-enhanced chest CT image from an 11-year-old HIV + male shows a well-defined solid mass in the right suprahilar peribronchial region

Imaging Features

The tumors have a propensity for the gastrointestinal tract and tracheobronchial tree and typically present as single or multiple well-defined solid masses [68] (Fig. 8.8). Metastases are most frequently observed in the lungs, although brain metastases have also been described [65].

Molecular Genetics

The molecular mechanism for development of EBV-related smooth muscle tumors is unclear, but there may be a relationship with expression of the EBV receptor CD21 [69]. Clonality studies indicate that multifocality of these lesions is caused by infection of multiple cells and not metastasis [70].

Pathology

EBV-related smooth muscle tumors consist of spindle cells with a smooth muscle phenotype, i.e., abundant cytoplasmic microfilaments (smooth muscle actin), elongated cells with squared-off nuclei, and expression of actin, desmin, and h-caldesmon. The tumor cells appear well differentiated with mild atypia and a variable amount of myxoid stroma. Mitotic activity can vary from none to 18/10 hpfs. Some cases contain intratumoral lymphocytes, and small round cell foci may be seen [70].

Prognostic Features

EBV-related smooth muscle tumors appear to be less aggressive than sporadic leiomyosarcomas, although recurrence is reported. Surgical excision, chemotherapy, cessation of immunotherapy (in transplant patients), or a combination thereof are standard treatment options. Because of their relatively indolent behavior, some prefer the term "smooth muscle tumor of uncertain malignant potential" [70].

Inflammatory Myofibroblastic Tumor (IMT)

Definition

A low-grade myofibroblastic tumor of borderline malignant potential occurring at a variety of sites in younger patients.

Clinical Features and Epidemiology

IMT has been referred to by a variety of names including inflammatory pseudotumor and plasma cell granuloma [7]. The current nomenclature emphasizes the dominant fibrous and muscular components of this tumor.

IMT is a rare neoplasm accounting for only 0.4–1 % of primary lung tumors [71]. However, in the largest series to date of primary pediatric lung tumors it accounted for 12.5 % (48/383) of tumors, having a similar incidence to malignant lesions such as carcinoid, mucoepidermoid carcinoma, and pleuropulmonary blastoma [4]. The tumor also accounted for the majority (52 %) of benign primary tumors of the lung in this series, although it has since been reclassified as low grade or borderline malignant [4].

IMT has a wide age distribution ranging from 1 to 77 years with an average age of presentation of 29.5 years [71]. In children, this tumor tends to occur above 5 years of age [5]. There is no sex or racial predilection [5].

IMT can occur at a variety of sites. The abdomen is the most common, followed by the lung (22 %) [72]. The presentation depends largely on the site of tumor. Presentations of pulmonary IMT range from asymptomatic to respiratory symptoms to the constellation of fever, weight loss, anemia, thrombocytosis, and polyclonal hyperglobulinemia with elevated ESR [72].

Imaging Features

The imaging appearance is typically a well-circumscribed solitary pulmonary mass [71]. Upper lobe predominance has been described [73]. The mass ranges widely in size from 1 to 36 cm with an average size of 3 cm [7]. A majority (83 %) are parenchymal with the remainder (17 %) being endobronchial [4] (Fig. 8.9). They can be homogeneously or heterogeneously low in attenuation, and calcification or cavitation are rarely seen [71]. There is aggressive local invasion of the chest wall in 5–10 % [7]. On MRI, they are typically hypointense on T1-weighted images and variably hyperintense on T2-weighted images. They demonstrate mild heterogeneous enhancement after contrast administration that is typically more pronounced in the delayed phases [71].

There is a high incidence of local recurrence, especially with incompletely resected tumors [72]. Metastases are rare but have been documented to the lung, brain, liver, and bone. A recent series reported a 25 % incidence of developing CNS metastases [73].

Molecular Genetics

Up to 56 % of these patients demonstrate increased cytoplasmic expression of the receptor tyrosine kinase protein anaplastic lymphoma kinase (ALK) encoded by the *ALK1* gene on chromosome 2p, secondary to translocations and fusions with a variety of partner genes. When over-expressed, *ALK1* is associated with an increased rate of local recurrence, decreased metastatic disease, and overall improved prognosis. Partner genes in *ALK1* fusions include *TPM3, TPM4, CLTC, RANBP2*, and *ATIC* [72]. These genetic rearrangements appear to be more common in tumors of children than those of adults [74]. They overlap somewhat with similar fusions found in anaplastic large cell lymphoma [75].

Pathology

IMT is a spindle cell lesion containing variable amounts of inflammatory cells, particularly eosinophils, lymphocytes, and plasma cells (hence the former name of "plasma cell granuloma")

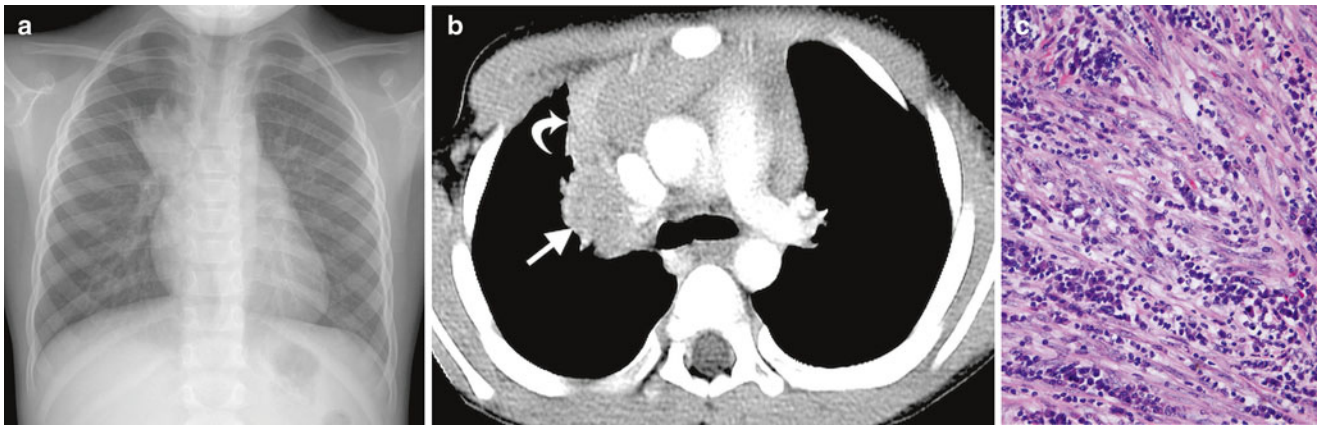

Fig. 8.9 Inflammatory myofibroblastic tumor. A chest radiograph (**a**) from a 4-year-old male shows a right suprahilar mass and volume loss of the right upper lobe. An axial contrast-enhanced chest CT image (**b**) reveals a low-attenuation non-calcified mass (*straight arrow*) along the region of the central right upper lobe bronchus with associated anterior right upper lobe atelectasis (*curved arrow*). Histology (**c**) of another case reveals a mixture of spindle cells and inflammatory cells, particularly plasma cells

(Fig. 8.9). The constituent tumor cells contain moderate amounts of cytoplasm with tapered cellular margins. They display variable eosinophilia, but not to the extent of rhabdomyosarcoma. Because of RNA content, a purplish tint may be apparent. The nuclei appear oval to elongated and show mild-to-moderate degrees of pleomorphism. The mitotic rate is variable and can be fairly brisk, and atypical mitoses may be seen. Occasional ganglion cell-like elements may be present [72].

Depending on a degree on the relative content of inflammatory cells, IMTs form three patterns: inflammatory, hemangiopericytomatous, and fibrous. The first pattern displays relatively a more fascicular arrangement with a diffuse inflammatory infiltrate. The hemangiopericytomatous pattern shows relatively loose cellularity enmeshed in a staghorn, granulation tissue-like vascularity. The fibrous pattern exhibits scar-like features, with more abundant collagen and relatively sparse inflammation.

Like most myofibroblastic lesions, IMTs express vimentin, actin, and occasionally desmin. Anti-α-smooth muscle actin shows strongest expression among the actin subtypes. ALK1 immunostaining, the best method for detecting the presence of *ALK1* fusions, is present in the majority of cases [76]. In ALK1-negative cases, FISH testing may indicate *ALK1* rearrangement [73]. ALK1-negative tumors may be associated with aneuploidy and more aggressive behavior [77].

Prognostic Features

IMTs usually act in a relatively indolent fashion, although about one-fourth recur, depending on site, adequacy of excision, and multinodularity. When over-expressed *ALK1* may be associated with an increased rate of local recurrence, decreased metastatic disease, and overall improved prognosis. Metastases are rare, occurring in <2 % of patients. Metastatic disease is associated with fusion negativity, with specific fusions such as *ALK1-RANBP2*, and with round cell cytology. Size, cellularity, and histological features are not predictive of outcome [72].

Congenital Peribronchial Myofibroblastic Tumor (CPMT)

Definition

A locally invasive tumor of the pluripotent mesenchyme surrounding the developing bronchi.

Clinical Features and Epidemiology

Congenital peribronchial myofibroblastic tumor (CPMT) has been previously described as massive congenital malformation of lung, hamartoma of lung, bronchopulmonary leiomyosarcoma, and primary bronchopulmonary fibrosarcoma [78]. The cellular nature of the tumor has led to confusion with malignant congenital pulmonary tumors. The current terminology is preferred to emphasize the benign histology of this lesion. The tumor is thought to develop at approximately 12 weeks of gestational age and have various degrees of smooth muscle and cartilaginous differentiation [79].

CPMT is very rare with approximately 25 cases reported in the literature [5] and the largest case series detailing 11 patients [80]. The mass is typically detected in the neonatal period, and prenatal detection has also been reported [80].

Although histologically benign, high mortality is reported predominantly secondary to nonimmune hydrops fetalis (55 % mortality). No sex or racial predilection, or syndromic, genetic, or maternal associations have been identified [78].

Imaging Features

CPMT typically appears as a large solitary well-defined pulmonary mass. Any lobe can be involved. The tumors are typically 5–7 cm in diameter and occupy much of the involved hemithorax, exerting mass affect with mediastinal shift [78]. Mass effect leads to hydrops fetalis in 36 % of cases [80]. Polyhydramnios is observed in 27 % of cases, presumably secondary to compression of the esophagus [80]. The tumor is heterogeneously hyperechoic on ultrasound [80], and heterogeneous but without cystic areas or calcification on CT [78]. The appearance on MRI has not been described. No local recurrence or metastasis has been reported [80].

Molecular Genetics

The genetics of CPMT are not well described. Some have complex karyotypic rearrangements [81]. A few cases published as CPMT show the t(12;15) and *TEL-TRK3* fusion of infantile fibrosarcoma [82], suggesting that, like cellular mesoblastic nephroma, at least some examples comprise visceral examples of this soft-tissue neoplasm, and the cellular features and typical age support this notion.

Pathology

CPMT typically occurs as a peribronchial mass containing interlacing fascicles of myofibroblastic cells. Tumor may also infiltrate interlobular septa and the subpleural region. The cells show a partial smooth muscle phenotype, such as smooth muscle actin expression and submicroscopic cytoplasmic microfilaments, which led to its early description as "leiomyosarcoma of lung." Although it has bland cytological features, mitotic activity can be brisk, and rare atypical forms may be seen, along with geographic necrosis. Some lesions have a minor cartilaginous component that increases markedly after birth [81]. One lesion to consider in the differential diagnosis is myofibroma, a benign mesenchymal disorder thought to be the most common fibrous tumor of infancy. In its visceral form, it often affects the lung and acts similar to a malignant neoplasm, although multifocality rather than metastasis likely accounts for the aggressive behavior [83].

Prognostic Features

In general, patients survive CPMT following surgical extirpation. However, some die in the prenatal or neonatal period as a result of fetal hydrops or respiratory failure [81].

References

1. Guillerman RP, McCarville ME, Kaste SC, Shulkin BL, Voss SD. Imaging studies in the diagnosis and management of pediatric malignancies. In: Poplack PD, Pizzo PA, editors. Principles and practice of pediatric oncology. Baltimore: Lippincott, Williams and Wilkins; 2011. p. 216–78.
2. Cohen MC, Kaschula RO. Primary pulmonary tumors in childhood: a review of 31 years' experience and the literature. Pediatr Pulmonol. 1992;14:222–32.
3. Hartman GE, Shochat SJ. Primary pulmonary neoplasms of childhood: a review. Ann Thorac Surg. 1983;36:108–19.
4. Hancock BJ, Di Lorenzo M, Youssef S, et al. Childhood primary pulmonary neoplasms. J Pediatr Surg. 1993;28:1133–6.
5. Dishop MK, Kuruvilla S. Primary and metastatic lung tumors in the pediatric population: a review and 25-year experience at a large children's hospital. Arch Pathol Lab Med. 2008;132:1079–103.
6. Yu DC, Grabowski MJ, Kozakewich HP, et al. Primary lung tumors in children and adolescents: a 90-year experience. J Pediatr Surg. 2010;45:1090–5.
7. Yousem S, Tazelaar H, Manabe T, et al. Inflammatory myofibroblastic tumor. In: Travis WD, Brambilla E, Muller-Hermelink HK, Harris CC, editors. World Health Organization classification of tumours: pathology and genetics of tumors of the lung, pleura, thymus, and heart. Lyon: IARC Press; 2004. p. 105–6.
8. McCahon E. Lung tumours in children. Paediatr Respir Rev. 2006;7:191–6.
9. Naffaa LN, Donnelly LF. Imaging findings in pleuropulmonary blastoma. Pediatr Radiol. 2005;35:387–91.
10. Lal DR, Clark I, Shalkow J, et al. Primary epithelial lung malignancies in the pediatric population. Pediatr Blood Cancer. 2005;45:683–6.
11. Roby BB, Drehner D, Sidman JD. Pediatric tracheal and endobronchial tumors: an institutional experience. Arch Otolaryngol Head Neck Surg. 2011;137:925–9.
12. Newman B. Thoracic neoplasms in children. Radiol Clin North Am. 2011;49:633–64.
13. McCarville MB, Lederman HM, Santana VM, et al. Distinguishing benign from malignant pulmonary nodules with helical chest CT in children with malignant solid tumors. Radiology. 2006;239:514–20.
14. Rosenfield NS, Keller MS, Markowitz RI, et al. CT differentiation of benign and malignant lung nodules in children. J Pediatr Surg. 1992;27:459–61.
15. Kuhns LR, Roubal S. Should intravenous contrast be used for chest CT in children with nonlymphomatous extrathoracic malignancies? Pediatr Radiol. 1995;25 Suppl 1:S184–6.
16. Kleis M, Daldrup-Link H, Matthay K, et al. Diagnostic value of PET/CT for the staging and restaging of pediatric tumors. Eur J Nucl Med Mol Imaging. 2009;36:23–36.
17. Weldon CB, Shamberger RC. Pediatric pulmonary tumors: primary and metastatic. Semin Pediatr Surg. 2008;17:17–29.
18. Lantuejoul S, Nicholson AG, Sartori G, et al. Mucinous cells in type 1 pulmonary congenital cystic adenomatoid malformation as mucinous bronchioloalveolar carcinoma precursors. Am J Surg Pathol. 2007;31:961–9.
19. French CA. NUT midline carcinoma. Cancer Genet Cytogenet. 2010;203:16–20.
20. Stelow EB, French CA. Carcinomas of the upper aerodigestive tract with rearrangement of the nuclear protein of the testis (NUT) gene (NUT midline carcinomas). Adv Anat Pathol. 2009;16:92–6.
21. den Bakker MA, Beverloo BH, van den Heuvel-Eibrink MM, et al. NUT midline carcinoma of the parotid gland with mesenchymal differentiation. Am J Surg Pathol. 2009;33:1253–8.

22. French CA, Kutok JL, Faquin WC, et al. Midline carcinoma of children and young adults with NUT rearrangement. J Clin Oncol. 2004;22:4135–9.
23. Mertens F, Wiebe T, Adlercreutz C, et al. Successful treatment of a child with t(15;19)-positive tumor. Pediatr Blood Cancer. 2007;49: 1015–7.
24. Polsani A, Braithwaite KA, Alazraki AL, et al. NUT midline carcinoma: an imaging case series and review of literature. Pediatr Radiol. 2012;42:205–10.
25. Kubonishi I, Takehara N, Iwata J, et al. Novel t(15;19)(q15;p13) chromosome abnormality in a thymic carcinoma. Cancer Res. 1991;51:3327–8.
26. Hammar SP, Brambilla C, Pugatch B, Geisinger K, Fernandez EA, Vogt P, Petrovitchev N, Matsuno Y, Aisner S, Rami-Porta R, Capelozzi VL, Schmidt R, Carvalho L, Petersen I, Gazdar A, Meyerson M, Hanash SM, Jen J, Harris CC. Squamous cell carcinoma. In: Travis WD, Brambilla E, Muller-Hermelink HK, Harris CC, editors. WHO classification of tumours: pathology and genetics of tumors of the lung, pleura, thymus, and heart. Lyon: IARC Press; 2004. p. 26–30.
27. Cook JR, Hill DA, Humphrey PA, et al. Squamous cell carcinoma arising in recurrent respiratory papillomatosis with pulmonary involvement: emerging common pattern of clinical features and human papillomavirus serotype association. Mod Pathol. 2000;13: 914–8.
28. Katz SL, Das P, Ngan BY, et al. Remote intrapulmonary spread of recurrent respiratory papillomatosis with malignant transformation. Pediatr Pulmonol. 2005;39:185–8.
29. Williams SD, Jamieson DH, Prescott CA. Clinical and radiological features in three cases of pulmonary involvement from recurrent respiratory papillomatosis. Int J Pediatr Otorhinolaryngol. 1994;30:71–7.
30. Pipavath SN, Manchanda V, Lewis DH, et al. 18F FDG-PET/CT findings in recurrent respiratory papillomatosis. Ann Nucl Med. 2008;22:433–6.
31. Gall T, Kis A, Tatar TZ, et al. Genomic differences in the background of different severity in juvenile-onset respiratory papillomatoses associated with human papillomavirus type 11. Med Microbiol Immunol. 2013;202(5):353–63.
32. Rabah R, Lancaster WD, Thomas R, et al. Human papillomavirus-11-associated recurrent respiratory papillomatosis is more aggressive than human papillomavirus-6-associated disease. Pediatr Dev Pathol. 2001;4:68–72.
33. Beasley MB, Thunnissen FB, Hasleton PS, Barbareschi M, Pugatch B, Geisinger K, Brambilla E, Gazdar A, Travis WD. Carcinoid tumour. In: Travis WD, Brambilla E, Muller-Hermelink HK, Harris CC, editors. World Health Organization classification of tumours: pathology and genetics of tumors of the lung, pleura, thymus, and heart. Lyon: IARC Press; 2004. p. 59–62.
34. Al-Qahtani AR, Di Lorenzo M, Yazbeck S. Endobronchial tumors in children: institutional experience and literature review. J Pediatr Surg. 2003;38:733–6.
35. Jeung MY, Gasser B, Gangi A, et al. Bronchial carcinoid tumors of the thorax: spectrum of radiologic findings. Radiographics. 2002;22:351–65.
36. Chong S, Lee KS, Chung MJ, et al. Neuroendocrine tumors of the lung: clinical, pathologic, and imaging findings. Radiographics. 2006;26:41–57. discussion 57–8.
37. Hervas Benito I, Bello Arques P, Loaiza JL, et al. Somatostatin receptor scintigraphy in pediatric bronchial carcinoid tumor. Rev Esp Med Nucl. 2010;29:25–8.
38. Swarts DR, Ramaekers FC, Speel EJ. Molecular and cellular biology of neuroendocrine lung tumors: evidence for separate biological entities. Biochim Biophys Acta. 1826;2012:255–71.
39. Rizzardi G, Marulli G, Calabrese F, et al. Bronchial carcinoid tumours in children: surgical treatment and outcome in a single institution. Eur J Pediatr Surg. 2009;19:228–31.
40. Brandwein MS, Ivanov K, Wallace DI, et al. Mucoepidermoid carcinoma: a clinicopathologic study of 80 patients with special reference to histological grading. Am J Surg Pathol. 2001;25:835–45.
41. Kim TS, Lee KS, Han J, et al. Mucoepidermoid carcinoma of the tracheobronchial tree: radiographic and CT findings in 12 patients. Radiology. 1999;212:643–8.
42. Wu M, Wang Q, Xu XF, et al. Bronchial mucoepidermoid carcinoma in children. Thorac Cardiovasc Surg. 2011;59:443–5.
43. Neville HL, Hogan AR, Zhuge Y, et al. Incidence and outcomes of malignant pediatric lung neoplasms. J Surg Res. 2009;156: 224–30.
44. Elnayal A, Moran CA, Fox PS, et al. Primary salivary gland-type lung cancer: imaging and clinical predictors of outcome. Am J Roentgenol. 2013;201:W57–63.
45. Xi JJ, Jiang W, Lu SH, et al. Primary pulmonary mucoepidermoid carcinoma: an analysis of 21 cases. World J Surg Oncol. 2012;10:232.
46. Manivel JC, Priest JR, Watterson J, et al. Pleuropulmonary blastoma. The so-called pulmonary blastoma of childhood. Cancer. 1988;62:1516–26.
47. Priest JR, McDermott MB, Bhatia S, et al. Pleuropulmonary blastoma: a clinicopathologic study of 50 cases. Cancer. 1997;80: 147–61.
48. Miniati DN, Chintagumpala M, Langston C, et al. Prenatal presentation and outcome of children with pleuropulmonary blastoma. J Pediatr Surg. 2006;41:66–71.
49. Priest JR. Pleuropulmonary blastoma. In: Schneider DT, Brecht IB, Olson TA, Ferrari A, editors. Rare tumors in children and adolescents, pediatric oncology. Berlin: Springer; 2012. p. 213–21.
50. Priest JR, Watterson J, Strong L, et al. Pleuropulmonary blastoma: a marker for familial disease. J Pediatr. 1996;128:220–4.
51. Schultz KA, Pacheco MC, Yang J, et al. Ovarian sex cord-stromal tumors, pleuropulmonary blastoma and DICER1 mutations: a report from the International Pleuropulmonary Blastoma Registry. Gynecol Oncol. 2011;122:246–50.
52. Dehner LP. Pleuropulmonary blastoma is THE pulmonary blastoma of childhood. Semin Diagn Pathol. 1994;11:144–51.
53. Oliveira C, Himidan S, Pastor AC, et al. Discriminating preoperative features of pleuropulmonary blastomas (PPB) from congenital cystic adenomatoid malformations (CCAM): a retrospective, age-matched study. Eur J Pediatr Surg. 2011;21:2–7.
54. Goel P, Panda S, Srinivas M, et al. Pleuropulmonary blastoma with intrabronchial extension. Pediatr Blood Cancer. 2010;54:1026–8.
55. Priest JR, Andic D, Arbuckle S, et al. Great vessel/cardiac extension and tumor embolism in pleuropulmonary blastoma: a report from the International Pleuropulmonary Blastoma Registry. Pediatr Blood Cancer. 2011;56:604–9.
56. Priest JR, Magnuson J, Williams GM, et al. Cerebral metastasis and other central nervous system complications of pleuropulmonary blastoma. Pediatr Blood Cancer. 2007;49:266–73.
57. de Krijger RR, Claessen SM, van der Ham F, et al. Gain of chromosome 8q is a frequent finding in pleuropulmonary blastoma. Mod Pathol. 2007;20:1191–9.
58. Hill DA, Ivanovich J, Priest JR, et al. DICER1 mutations in familial pleuropulmonary blastoma. Science. 2009;325:965.
59. Dehner LPWJ, Watterson J, Priest JR. Pleuropulmonary blastoma. A unique intrathoracic-pulmonary neoplasm of childhood. Perspect Pediatr Pathol. 1995;18:214–26.
60. Reichman M, Kovanlikaya A, Mathew S, et al. Pulmonary blastoma in a neonate: a lesion distinct from pleuropulmonary blastoma with unique cytogenetic features. Pediatr Radiol. 2010;40:366–70.
61. Agrawal D, Lahiri TK, Lakhotia S, et al. Pulmonary blastoma in a young adult. Indian J Chest Dis Allied Sci. 2012;54:189–92.
62. Indolfi P, Bisogno G, Casale F, et al. Prognostic factors in pleuropulmonary blastoma. Pediatr Blood Cancer. 2007;48:318–23.
63. Dishop MK, McKay EM, Kreiger PA, et al. Fetal lung interstitial tumor (FLIT): a proposed newly recognized lung tumor of infancy

to be differentiated from cystic pleuropulmonary blastoma and other developmental pulmonary lesions. Am J Surg Pathol. 2010;34:1762–72.
64. Lazar DA, Cass DL, Dishop MK, et al. Fetal lung interstitial tumor: a cause of late gestation fetal hydrops. J Pediatr Surg. 2011;46:1263–6.
65. Chadwick EG, Connor EJ, Hanson IC, et al. Tumors of smooth-muscle origin in HIV-infected children. JAMA. 1990;263:3182–4.
66. McClain KL, Leach CT, Jenson HB, et al. Association of Epstein-Barr virus with leiomyosarcomas in children with AIDS. N Engl J Med. 1995;332:12–8.
67. Lee ES, Locker J, Nalesnik M, et al. The association of Epstein-Barr virus with smooth-muscle tumors occurring after organ transplantation. N Engl J Med. 1995;332:19–25.
68. Balsam D, Segal S. Two smooth muscle tumors in the airway of an HIV-infected child. Pediatr Radiol. 1992;22:552–3.
69. Suzuki K, Urushihara N, Fukumoto K, et al. A case of Epstein-Barr virus-associated pulmonary leiomyosarcoma arising five year after a pediatric renal transplant. Pediatr Transplant. 2011;15:E145–8.
70. Parham DM, Alaggio R, Coffin CM. Myogenic tumors in children and adolescents. Pediatr Dev Pathol. 2012;15:211–38.
71. Takayama Y, Yabuuchi H, Matsuo Y, et al. Computed tomographic and magnetic resonance features of inflammatory myofibroblastic tumor of the lung in children. Radiat Med. 2008;26:613–7.
72. Coffin CM, Hornick JL, Fletcher CD. Inflammatory myofibroblastic tumor: comparison of clinicopathologic, histologic, and immunohistochemical features including ALK expression in atypical and aggressive cases. Am J Surg Pathol. 2007;31:509–20.
73. Siminovich M, Galluzzo L, Lopez J, et al. Inflammatory myofibroblastic tumor of the lung in children: anaplastic lymphoma kinase (ALK) expression and clinico-pathological correlation. Pediatr Dev Pathol. 2012;15:179–86.
74. Gleason BC, Hornick JL. Inflammatory myofibroblastic tumours: where are we now? J Clin Pathol. 2008;61:428–37.
75. Gascoyne RD, Lamant L, Martin-Subero JI, et al. ALK-positive diffuse large B-cell lymphoma is associated with Clathrin-ALK rearrangements: report of 6 cases. Blood. 2003;102:2568–73.
76. Cook JR, Dehner LP, Collins MH, et al. Anaplastic lymphoma kinase (ALK) expression in the inflammatory myofibroblastic tumor: a comparative immunohistochemical study. Am J Surg Pathol. 2001;25:1364–71.
77. Coffin CM, Patel A, Perkins S, et al. ALK1 and p80 expression and chromosomal rearrangements involving 2p23 in inflammatory myofibroblastic tumor. Mod Pathol. 2001;14:569–76.
78. Travis W, Dehner LP, Manabe T, et al. Congenital peribronchial myofibroblastic tumor. In: Travis WD, Brambilla E, Mɶller-Hermelink HK, Harris CC, editors. World Health Organization classification of tumours: pathology and genetics of tumors of the lung, pleura, thymus, and heart. Lyon: IARC Press; 2004. p. 102–3.
79. Alobeid B, Beneck D, Sreekantaiah C, et al. Congenital pulmonary myofibroblastic tumor: a case report with cytogenetic analysis and review of the literature. Am J Surg Pathol. 1997;21:610–4.
80. Horikoshi T, Kikuchi A, Matsumoto Y, et al. Fetal hydrops associated with congenital pulmonary myofibroblastic tumor. J Obstet Gynaecol Res. 2005;31:552–5.
81. Huppmann AR, Coffin CM, Hoot AC, et al. Congenital peribronchial myofibroblastic tumor: comparison of fetal and postnatal morphology. Pediatr Dev Pathol. 2011;14:124–9.
82. Steelman C, Katzenstein H, Parham D, et al. Unusual presentation of congenital infantile fibrosarcoma in seven infants with molecular-genetic analysis. Fetal Pediatr Pathol. 2011;30:329–37.
83. Koujok K, Ruiz RE, Hernandez RJ. Myofibromatosis: imaging characteristics. Pediatr Radiol. 2005;35:374–80.